NUCL SCI TECH (2020) 31:43
https://doi.org/10.1007/s41365-020-00754-1

Electroplating titanium film on 316L stainless steel in LiCl–KCl–Ti^{x+} ($2 < x < 3$) molten salts

Jun-Xia Liu[1,2] · Jing-Chun Liu[2,3] · De-Wu Long[2,4] · Ke Zhan[1]

Received: 24 December 2019 / Revised: 22 February 2020 / Accepted: 23 February 2020 / Published online: 22 April 2020

Abstract To improve the anti-corrosion properties of 316L stainless steel, titanium (Ti) metal films were electroplated on it using LiCl–KCl molten salts as the electrolyte, and low-valence Ti^{x+} ($2 < x < 3$) as the solute. The solute was produced by the reaction of Ti^{4+} and Ti^0 via mixing K_2TiF_6, and Ti metal (sponge Ti) in the melts. Anti-corrosion test has shown significant enhancement in the stability of the Ti-coated 316L due to the presence of Ti film. However, the anti-corrosion properties did not enhance with an increase in the thickness of the Ti layers owing to a possible defect in the thicker Ti layers.

Keywords Molten salts · Electro-plating · Ti coating · Anti-corrosion

This work was supported by the "Strategic Priority Research Program'' Chinese Academy of Sciences (No. XDA02020000), Transformational Technologies for Clean Energy and Demonstration (No. XD21081200), and K.C. Wong Education Foundation (No. GJTD-2018-10).

✉ De-Wu Long
longdewu@sinap.ac.cn

✉ Ke Zhan
zhanke@usst.edu.cn

[1] School of Material Science and Engineering, University of Shanghai for Science and Technology, Shanghai 200093, China

[2] Department of Molten Salt Chemistry and Engineering, Shanghai Institute of Applied Physics, Chinese Academy of Sciences, Shanghai 201800, China

[3] University of Chinese Academy of Sciences, Beijing 100049, China

[4] Key Laboratory of Interfacial Physics and Technology, Chinese Academy of Sciences, Shanghai 201800, China

1 Introduction

To improve the anti-corrosion properties of 316L stainless steel, electroplating of stainless steel with refractory metal film [1, 2], such as chromium (Cr) or titanium (Ti), in high-temperature eutectic salts has been extensively adopted for decades [3–5]. In contrast to the sophisticated Cr plating, Ti film plating is still a challenge because: (1) The electrochemical behavior of high-valent Ti ions (Ti^{4+}, Ti^{3+}) is complicated, and thus the stepwise reduction process often involves reversible intermediate states [6], which in turn reduces the deposition current efficiency and, consequently, the economic competence. (2) Various valent states of Ti ions (Ti^{4+}, Ti^{3+}, and Ti^{2+}) have been reported to be stable in various molten salts [7–9], and such low-valence intermediate states are usually converted along with the experimental conditions such as the composition of the salts, and the temperature. Therefore, it is hard to obtain Ti films with uniform with uniform morphologies using a single deposition parameter because the electrolyte varies during the deposition period [10]. (3) The Ti ions and Ti metals underwent feasible disproportionation reactions, which consumes the deposited Ti metal, thus deteriorating the morphology of the plated film [11]. Therefore, Ti product is obtained in powdered or dendritic phases rather than dense and well-stacked films in most cases [12]. The absence of a dense Ti layer generally results in the loss of anti-corrosion properties [13].

Several studies have been conducted to investigate the electrochemical reaction mechanism of various Ti ions in different kinds of molten salts [14–19]. Ti^{4+} has been reported to be stable in chlorides and fluorides as hexa-halogen coordinated states (i.e., $TiCl_6^{2-}$ or TiF_6^{2-}) by using the raw materials $TiCl_4$ and K_2TiF_6, respectively

[20, 21]. It has been proven that the reduction of Ti^{4+} to metal consisted of two pathways, either via reactions (1) and (4) or via reactions (1), (2), (3), and (6). In addition, the compositions of the molten salts were confirmed to have comprehensive influence on the Ti^{4+} reduction process. For example, the increase in F^- in the LiCl–KCl molten salts promoted the former two-step reaction mechanism via Ti^{3+} as intermediate [22]. Meanwhile, the later reduction process via reaction (2) occurred in pure chloride melt by using $TiCl_4$ as the raw material. Moreover, such tetravalent species were easily reduced to low-valence states due to the presence of reductants such as metallic Ti or graphite in the melts [23, 24]. The presence of fluoride ions and large-radii alkali ions (e.g., Cs^+) [25] in the molten salts was reported to stabilize the trivalent ion (Ti^{3+}), while the chloride ion and Li^+ [8] were regarded as feasible for stabilizing Ti^{2+}. Although Ti^{3+} was found dominant in the pure fluoride salts (LiF–NaF–KF, LiF–BeF_2), the main intermediate in chloride salts (LiCl–KCl, LiCl–$AlCl_3$) was Ti^{2+}. Furthermore, elevating the experimental temperature was favorable for transformation of Ti^{2+} to Ti^{3+} in chlorides.

The reactions of various species of Ti ions in the melts:

$$Ti^{4+} + e^- \rightarrow Ti^{3+} \quad (1)$$

$$Ti^{3+} + e^- \rightarrow Ti^{2+} \quad (2)$$

$$Ti^{2+} + 2e^- \rightarrow Ti^0 \quad (3)$$

$$Ti^{3+} + 3e^- \rightarrow Ti^0 \quad (4)$$

$$2Ti^{4+} + Ti^0 \rightarrow 2Ti^{3+} + Ti^{2+} \quad (5)$$

$$2Ti^{3+} + Ti^0 \rightarrow 3Ti^{2+} \quad (6)$$

$$Ti^{4+} + Ti^0 \rightarrow 2Ti^{2+} \quad (7)$$

$$3Ti^{4+} + Ti^0 \rightarrow 4Ti^{3+} \quad (8)$$

Despite the complications in electrode reaction, several studies have focused on production of Ti metal in molten salt mediums [26–29]. However, only a few studies have been conducted on the fabrication of dense Ti coating layer. The investigation of the electrode reactions of the Ti deposition process revealed that the morphology of the obtained films correlated with both the initial valance of Ti ion and the composition of molten salts [30, 31]. It has been reported that the initial Ti^{4+} and Ti^{3+} undergo multiple reduction steps before the formation of Ti metal. The inevitable reaction between high-valence ions (Ti^{4+} or Ti^{3+}), and the deposited Ti metal further complicate the control of the morphology because such reactions continuously contribute to the consumption of the deposited Ti plated film. In the chloride molten salt, a feasible disproportionation reaction occurs between the $TiCl_4$ in the diffusion layer of the electrode and the deposited metal on the electrode, hindering further reduction of Ti as well as the diffusion process of low-valent Ti ions. Therefore, the morphology of the deposited Ti products was usually in powdered and dendritic phases [32]. At higher current density and/or extended deposition time, such isolating effect was intense, which further enhanced the powdered titanium formation [13, 33]. Two solutions were proposed to overcome these limitations, where one solution was to use higher concentration of low-valent Ti compound as the solute, which in turn decreased the diffusion barrier by increasing the gradient concentration of bulk solution and diffusion layer [24, 30]; the other was to apply low current density which can suppressed the generation of polarization on the electrode when titanium was deposited [34].

By adjusting the pH of the molten salt medium (e.g., by adding F^-), the disproportionation reaction caused by the reaction of Ti ion species or other reduction processes were excluded [33, 35]. The low-valent titanium concentration was reported to be 2–5%, and the valence ratio range was 2.2–2.4. The deposit obtained in this electrolyte was larger, and the Ti layer was stacked with uniform crystal grains in a sheet [24]. In addition, it also showed an increase in the size of the crystals with an increase in the deposition temperature, which further made the edges of the grains clearer [10, 30].

Additionally, investigations have revealed that the compositions of the molten salts, in particular, the species of halogen ions (F^-, Cl^-), and alkali ions (Cs^+, K^+), affected the electrode reactions because of the thermodynamic stability of the Ti ions owing to their strong coordination [7, 8, 36, 37]. Precisely, Ti ions have been reported to coordinate with Cl^- in chloride melts accompanied with alkali metal cations in the outer sphere, and these coordination clusters are affected by the composition of the molten salts. In chloride melts, when the initial ions are Ti^{4+}, the reduction process to metal titanium consisted of three steps (1), (2), and (3). Meanwhile, a two-step reduction, namely, (1) and (4), in the CsCl melt [22] was observed because the Cs^+ had a strong basic cation radius. It can easily combine with Cl^- in the chloride to affect the binding of the Ti ion to the chloride ion. Such reactions are controlled by Ti ions by instantaneous diffusion and charge transfer.

In the all-fluorides melt, Ti^{3+} or Ti^{4+} were present in a stable form of TiF_6^{3-} or TiF_6^{2-}, respectively. The reduction of Ti^{3+} to Ti^0 was a one-step process [38, 39]. However, in the case of the fluoride–chloride mixtures, the reaction (7) occurred when the TiF_6^{2-} melt concentration was less than 0.8 mol%; however, it was the reaction (8) which occurred while the concentration exceeded 2.8 mol%. In the melts containing high concentrations of fluoride, there was no intermediate valence state, and Ti^{2+} existed in the molten salt. As the content of TiF_6^{2-}

increased, $TiCl_y^{(y-4)-}$ was converted into a complex form of $TiF_x^{(x-4)-}$ by $TiF_xCl_y^{(x+y-4)-}$ [40–43].

To obtain a dense film, low-valent Ti ions such as Ti^{2+} and/or Ti^{3+} were used in a fixed-composition molten salt as the electrolyte, thereby avoiding the multiple steps of the reduction electrode process. In addition, applying constant current on the electrode was essential to exclude the possibility of fluctuation of the deposition process. Here, we have reported the preparation process of dense Ti plating film on 316L substrate by using LiCl–KCl–Ti^{x+} ($2 < x < 3$) solution, in which Ti^{x+} was synthesized by the reaction of Ti^{4+} and Ti metal in the melts. The generation of Ti^{x+} ions was characterized by various techniques. The deposition parameters were optimized, and a denser Ti film was obtained. The anti-corrosion property of the as-prepared Ti-coated 316L was evaluated by comparing it with raw 316L. The results implied a significant enhancement in the chemical stability after electroplating with Ti film.

2 Experimental method

2.1 Reagents and materials

Analytical-grade LiCl (99.8%), KCl (99.97%), K_2TiF_6 (99.99%), tungsten wire (99.5%, Φ1 mm), and graphite rod (99.5%, Φ2 mm) were purchased from Sinopharm Chemical Reagent Co., Ltd., and Ti sponge (99.7%, $\Phi < 25.4$ mm) was purchased from Alfa Industrial Inc., K_2TiF_6 (99.99%) and Ti sponge (99.7%, $\Phi < 25.4$ mm) were used directly without further purification.

2.2 Electrochemical measurements and electrodes

The eutectic LiCl–KCl molten salt was prepared by mixing LiCl and KCl in the molar ratio of 59:41, and the mixture was placed inside an alumina crucible. This crucible was loaded in a chamber of a resistance furnace (Fig. 1), that was connected to a glove box charged with argon (99.999%) to maintain the oxygen/water concentration of less than 10 ppm. The LiCl–KCl mixture was stepwise heated to 573 K for 3 h and was maintained at this temperature for 5 h to remove the absorbed humidity. Later, the temperature was raised to 823 K and was maintained for 1 h to melt the eutectic. Different concentrations of LiCl–KCl–Ti^{x+} salts were prepared by adding certain amounts of K_2TiF_6 (0.1–1.0 mol%), and an excess of Ti sponge into the LiCl–KCl molten salt at 823 K, and was maintained at this temperature for 1 h to complete the reaction between Ti^{4+} and Ti. The concentration of dissolved Ti ions in the melts was primarily determined using inductively coupled plasma–atomic emission spectroscopy (ICP–AES) measurement.

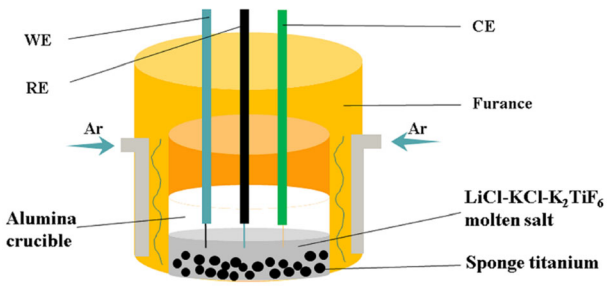

Fig. 1 (Color online) Schematic illustration of the layout of molten salt electrolytic cell

All electrochemical experiments were performed by Autolab PGSTAT302N with Nova 1.9 software. Three-electrode system was used for the electrochemical measurements. We used pure tungsten (W) wire (Φ1 mm) as the working electrode (WE) to investigate the electrochemical behavior of Ti^{x+} because W is regarded as an inert material. 316L stainless steel wire (Φ1 mm) was used as the working electrode for electroplating experiments. It was immersed in dilute nitric acid (0.1 mol%) for 30 min followed by ultrasonic cleaning with deionized water to remove the oxide layer from the surface. Graphite rod (Φ2 mm) or titanium wire (Φ1 mm) was used as counter electrode (CE). A homemade Ag/AgCl was used as the reference electrode (RE). Detailed description of the Ag/AgCl reference electrode has been published previously. In summary, we placed the mixture of LiCl–KCl and AgCl (5.0 mol%) in a BN tube, an Ag wire was immersed into the salt to serve as the electrode, and a tiny hole in the side of BN tube served as the ion tunnel.

2.3 Characterization and analysis

After electroplating, the WE was taken out from the molten salt and cooled in the glove box. Later, it underwent stepwise washing using deionized water and acetone to remove the adhesive salts. The washed samples were dried in a vacuum dry box overnight before further characterization. An energy-dispersive spectrometer (SEM–EDS, Zeless Merlin Compact LED 1530 VP) was used to investigate the micro-morphology and analyze the composition of the film. The XRD instrument model used was D8 Advance (Bruck, Germany). Samples of XRD were used to detect the elemental analysis of the coating. The contents of molten salt were characterized by ICP-AES.

3 Results and discussion

3.1 Electrochemical behavior of Ti

Synthesis of Ti^{x+} ($2 < x < 3$) by the reaction of Ti^{4+} and Ti metal in various molten salts has been extensively confirmed. The Ti^{x+} ions obtained by this reaction vary from case to case because the stability of Ti^{2+} or Ti^{3+} depends on both the composition of the molten salt and experimental conditions (e.g., temperatures). In order to identify the state of Ti^{x+} in our case, the melts from LiCl–KCl–K_2TiF_6–Ti were sampled at particular time intervals, and the samples were characterized using various techniques to deduce the evolution of Ti^{x+} ($2 < x < 3$) ions in this system.

ICP-AES was used to determine the concentration of dissolved Ti ions, and was found to be 5.2×10^{-3} mol L^{-1} for LiCl–KCl–Ti (5.0 mol%) after 16 h, 2.0 mol L^{-1} for LiCl–KCl–K_2TiF_6 (1.0 mol%)-Ti after 11 h, and 0.24 mol L^{-1} for LiCl–KCl–K_2TiF_6 (0.5 mol%) after 15 h, respectively (Table 1). The results showed that the dissolving concentration of Ti^0 metal in LiCl–KCl was very low (approximately 170 ppm), while the dissolution of Ti^{4+} (K_2TiF_6) reached saturation easily in LiCl–KCl–K_2TiF_6 (0.5 mol%) system. In contrast, the concentration of Ti^{x+} significantly increased as K_2TiF_6 and Ti metal were present together in the melts, and implied that the reaction between Ti^{4+} and Ti occurring in this case introduced extra Ti ions into the melts as the dissolved states. It should be noted that the concentration of Ti^{x+} in LiCl–KCl–K_2TiF_6 (1.0 mol%)-Ti was 10 times of that in LiCl–KCl–K_2TiF_6 (0.5 mol%), which further indicated the contribution of other reactions in introducing the Ti ions into the melts rather than reaction (5) because stoichiometric calculation from this reaction indicated that the concentrations of Ti^{x+} increased only by 67%. However, previous literatures indicated that not only Ti^{4+}, but also Ti^{3+} reacted with Ti metal to form low-valent Ti ions.

Figure 2 shows the cyclic voltammetry (CV) curves of LiCl–KCl–K_2TiF_6 (0.5 mol%)-Ti that were recorded after particular time intervals. The results obtained in LiCl–KCl–K_2TiF_6 (0.5 mol%) are also shown for comparison. Three couples of redox peaks were observed in LiCl–KCl–K_2TiF_6 (0.5 mol%) melts, which are marked as A/A′, B/B′, and C/C′, respectively. According to the previous works, one can easily assign A/A′ to $Ti^{4+} \rightarrow Ti^{3+}$, B/B′ to $Ti^{3+} \rightarrow Ti^{2+}$, and C/C′ to $Ti^{2+} \rightarrow Ti^0$. The CV curve of LiCl–KCl–K_2TiF_6 (0.5 mol%)-Ti evolve with time. Firstly, the disappearance of Ti^{4+} (A/A′) signal, and the simultaneous promotion of Ti^{3+} (B/B′) and Ti^{2+} (C/C′) peaks implies the reaction between Ti^{4+} and Ti^0 occurring in this system, which further depletes the Ti^{4+} ion while producing Ti^{3+}, Ti^{2+} in the melts. As the time increased, the signal of Ti^{2+} peak increased continuously accompanied with coinstantaneous suppressing of the signal of Ti^{3+}, indicating a shift from Ti^{3+} to Ti^{2+}. In fact, the dominance of reaction (6) in the system promotes the reduction of Ti^{4+} and Ti^{4+} ions were exhausted.

Figure 3 shows the time-dependent evolutional XPS patterns obtained for LiCl–KCl–K_2TiF_6 (0.5 mol%)-Ti. It can be inferred that Ti^{4+} and Ti^{3+} are the dominant species at 15 h. As the time elapsed, the signal of Ti^{4+} gradually decreased with an increase in the generated pattern of Ti^{2+}, implying the reaction between Ti^{4+} and sponge Ti to consume the Ti^{4+} and, consequently, form Ti^{2+}. Eventually, Ti^{4+} was exhausted and the only Ti species present in the system were Ti^{3+} and Ti^{2+}, in which the Ti^{2+} was the dominant one. The observations further confirmed the results of the CV experiments.

Table 1 ICP-AES results of sampled LiCl–KCl–Ti^{x+} melts after various reaction times

Molten salts	C_{con} (mol L^{-1})
LiCl–KCl–Ti	5.2×10^{-3} (16 h)
LiCl–KCl–K_2TiF_6	0.24 (15 h)
LiCl–KCl–K_2TiF_6–Ti	2.0 (11 h)

3.2 Electroplating Ti film on 316L matrix

After preparing Ti^{x+} electrolyte, the electrochemical experiments and deposition processes were carried out using a three-electrode system, in which a Ti wire was used as the counter electrode, a 316L stainless steel wire as the cathode, and Ag/AgCl molten salt as the reference electrode. Serial experiments were conducted at various conditions to evaluate the influence of deposition parameters such as applied current density, deposition time, and the temperature on the obtained Ti plated film (Figs. 4, 5, 6).

Figure 4 shows the SEM images of Ti obtained by applying different current densities at 773 K with fixed concentration of Ti^{x+} in the melts. A statistical study of these data revealed that the average sizes of the deposited Ti layer were equivalent (2.0 μm), although the applied current densities varied, revealing a weak correlation between the current densities and crystal sizes thus formed. Indeed, the morphology of the electrodeposited Ti has been reported to mainly depend on the nucleation rate. In given conditions, the nucleation rate depends on the concentrations of reactive Ti ions on the surface of the electrode rather than current density or temperatures. In turn, the concentrations of Ti ions in the bulk molten salt, and the applied current densities on the electrode resulted in the

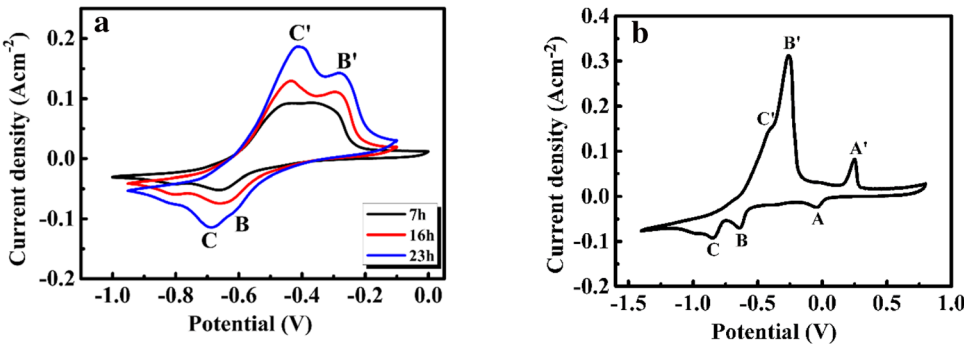

Fig. 2 (Color online) Cyclic voltammetry curves of **a** LiCl–KCl–K_2TiF_6 (0.5 mol%)-Ti, and **b** LiCl–KCl–K_2TiF_6 (0.5 mol%) at 823 K by using W as the working electrode. Scanning rate: 0.1 V s^{-1}, CE: graphite rod, RE: Ag/AgCl

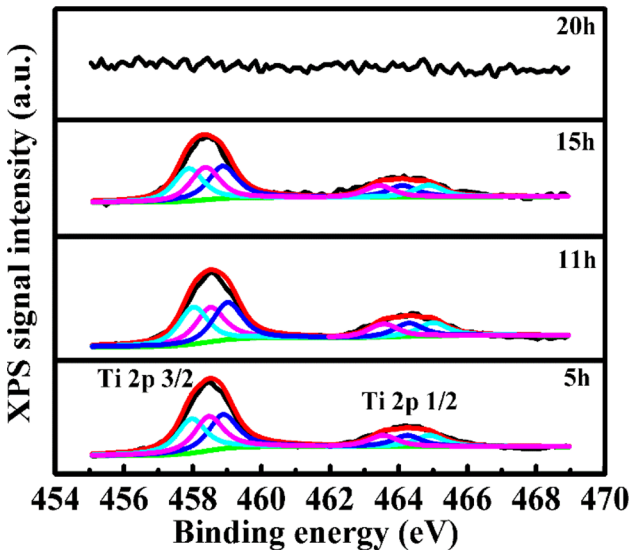

Fig. 3 (Color online) XPS spectrum of LiCl–KCl–K_2TiF_6 (0.5 mol%)-Ti molten salt with different reaction times under melting state at 823 K

rate of consumption of Ti ions in the diffusion layer near the electrode during the coating process [28].

In contrast, the granular average sizes were found to grow with a prolonged time (Fig. 5). The sizes were found to be 1.8 μm for a duration of 300 s and 600 s, while they were found to be 6.0 μm for a duration of 1200 s and 2400 s. The results indicated that longer deposition time was favorable for a layer composed with larger Ti particles. However, the sizes of Ti particles were distributed in two regions: small particles during the initial period, while large ones during the extended time. It has been previously reported that the orientation of deposited Ti depended on the initially formed nuclei [10]. The extended deposition time led to the orientational growth of initial nuclei into larger granular rather than new nuclei formation.

The influences of deposition temperatures on the obtained Ti crystal sizes were also evaluated (Fig. 6). The obtained particle size was 2.0 μm for 773 K, while it was 6.0 μm for 823 K, thus indicating the benefits of an elevated temperature for large particle formation.

In contrast to the deposition time, the current densities and temperatures were correlated directly to the electrode reaction and/or the stability of Ti^{x+} in the melts. More negative (higher) current densities exhibited a better reductive capability, and thus, higher density will easily cause the reduction of high-valent Ti ions in the melt, while lower-density environments are more conductive to the reduction of low-valent Ti ions. Actually, the Ti^{x+} in our study was in a metastable state. Therefore, a narrow range of applied current densities were available for tuning. In addition, the temperature has more complicated influences on the system. On the one hand, the temperature evaluation drives the reaction $Ti^{4+} \rightarrow Ti^{3+} \rightarrow Ti^{2+} \rightarrow Ti^{0}$ to the right. On the other hand, higher temperature was considered more feasible for the diffusion of Ti ions, and further favorable for the electrode reaction. Unfortunately, the temperature change in our case was limited by the physicochemical properties of the melts (723–873 K). When the temperature was more than 823 K, significant

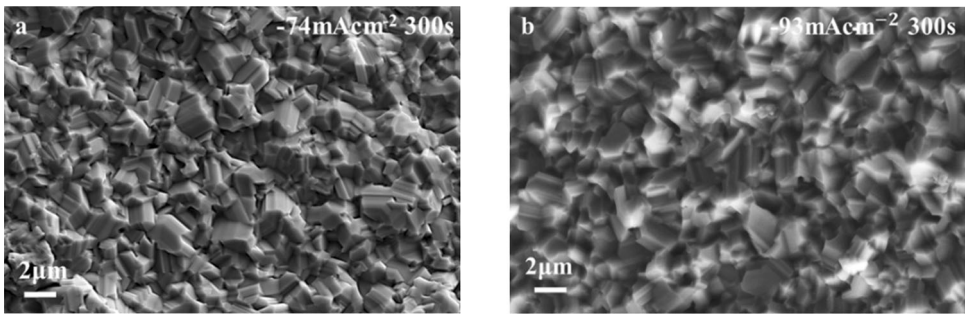

Fig. 4 SEM images of titanium films deposited for 300 s with various current densities **a** − 74 mA cm^{-2}, **b** − 93 mA cm^{-2}, in LiCl–KCl–K_2TiF_6 (1.0 mol%)-Ti at 773 K, WE: 316L SS, CE: titanium wire, RE: Ag/AgCl

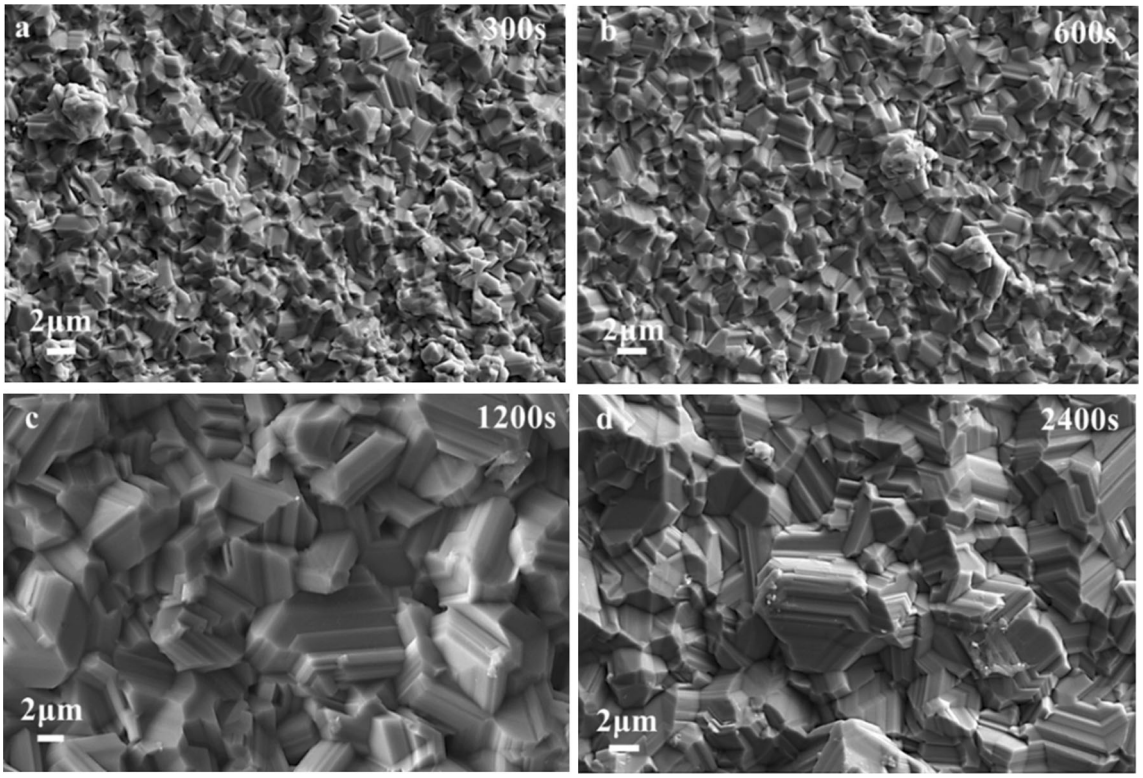

Fig. 5 SEM images of titanium films deposited by applying − 74 mA cm^{-2} current density with different deposited times **a** 300 s, **b** 600 s, **c** 1200 s, **d** 2400 s, in LiCl–KCl–K_2TiF_6 (1.0 mol%)-Ti at 773 K, WE: 316L SS, CE: titanium wire, RE: Ag/AgCl

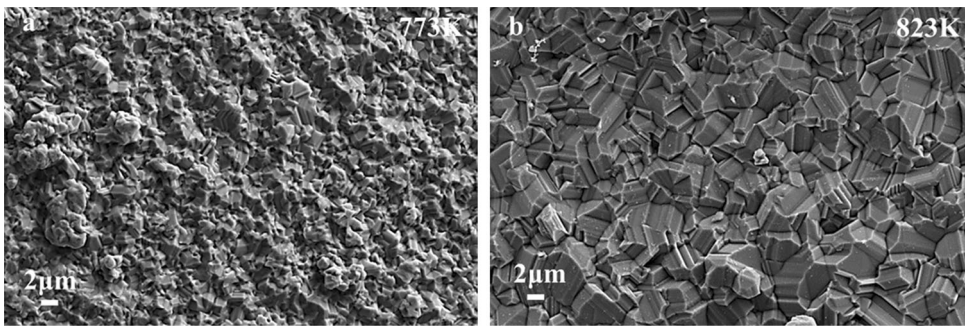

Fig. 6 SEM images of titanium films deposited on − 74 mA cm^{-2} for 300 s with different deposited temperatures **a** 773 K, **b** 823 K, in LiCl–KCl–K_2TiF_6 (1.0 mol%)-Ti, WE: 316L SS, CE: titanium wire, RE: Ag/AgCl

vaporization of melt components was observed which changed the compositions of this system subsequently.

The obtained Ti-plated 316L samples were cut out, and the EDS section model was used to analyze the thickness of the coating and the relationship between Ti layer and the substrate (Fig. 7). Interestingly, the thicknesses of the Ti layers were not linearly related to the deposition times. It was determined to be 5 μm for 300 s and 600 s, 17 μm for 1200 s, and 10 μm for 2400 s. Based on the observations, it is reasonable to deduce that the deposition process is composited of three stages. The nuclei formation and grain growth occurred at the initial stages (below 600 s). As discussed above, the nuclei formation depended on the reactive Ti ions and the applied current densities. In our case, equivalent thicknesses were observed in 300 s and 600 s because, although the formation of nuclei was equivalent, the prolonged time contributed to the growth of the granular for covering the substrate. After covering of the substrate was completed, new nuclei were formed on the initial Ti layer, and therefore, an increase in the Ti layer was observed with an increase in the time period (1200 s). At the extended stage, the possibility of consumption of Ti^{x+} near the electrode and the generation of high-valent Ti ions at the anode changed the composition of the melts. The high-valent Ti ions reacted with the deposited Ti layer of the cathode, and consequently, the Ti layer decreased as the time period increased (2400 s). Additionally, there is a possibility of potential defects that could be generated during such reactions, which would lead to the loss of anti-

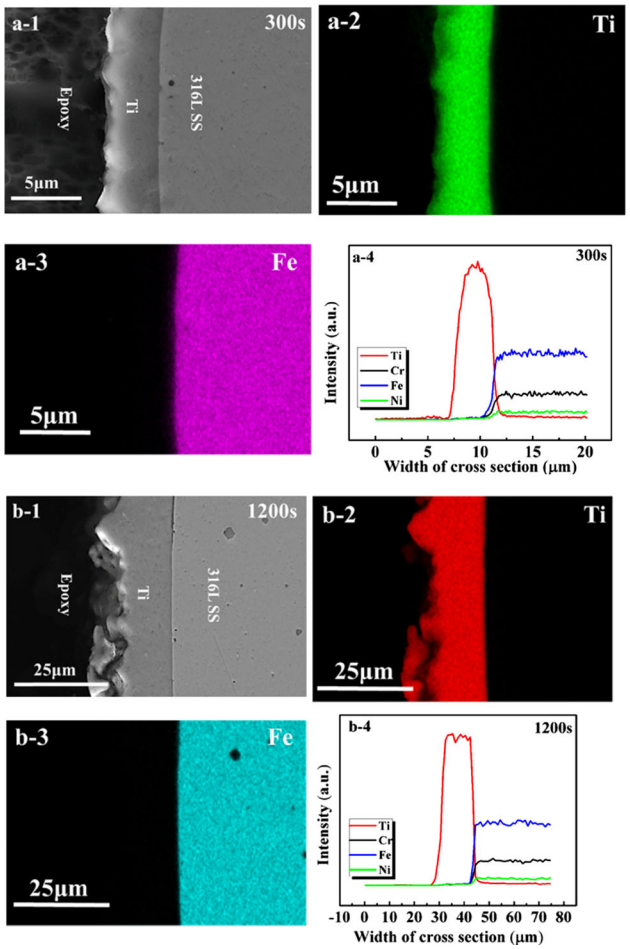

Fig. 7 (Color online) Cross-sectional characterization and EDS map scanning of titanium film on 316L substrate that was obtained at various conditions. **a** − 74 mA cm^{-2} for 300 s, **b** − 74 mA cm^{-2} for 1200 s at 773 K in LiCl–KCl–K_2TiF_6 (1.0 mol%)-Ti

corrosion properties, and is indicated by the following experiments.

Moreover, it was clearly shown that the Ti plated layer and the 316L substrate were connected by a Ti–Fe alloy inter-layer, and the thicknesses of the inter-layers changed with the deposition times (longer time indicated thicker connection layer).

3.3 Anti-corrosion behavior of Ti-coated 316L

The anti-corrosion behavior of the as-prepared Ti-coated 316L was evaluated using potential polarization dynamics method in a 3.5-wt% NaCl aqueous solution (Fig. 8). Table 2 shows the analytical results of the polarization curves. The corrosion potentials, which are regarded as an index for chemical stability, were observed to shift positively, indicating a significant improvement in the corrosion tolerance of Ti-coated 316L either for the 5 μm layer, 10 μm layer, or 17 μm layer. Meanwhile, the corrosion

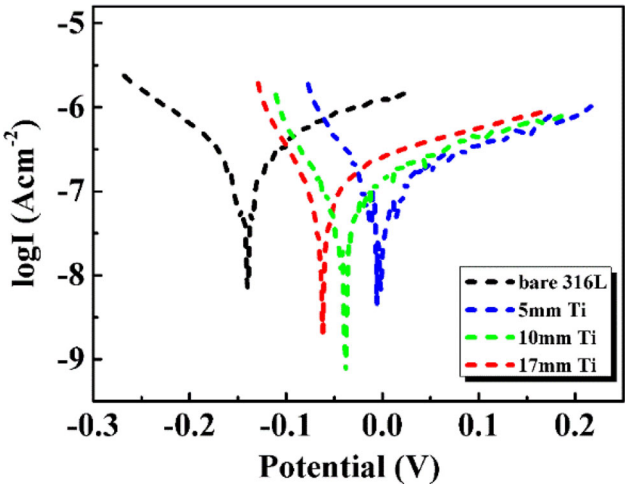

Fig. 8 (Color online) Polarization curves of raw 316L and Ti-coated 316L in 3.5-wt% NaCl solution at scanning rate of 1 mV s^{-1} (raw 316L; 5 μm Ti; 10 μm Ti; 17 μm Ti)

Table 2 Electrochemical parameters and calculated corrosion rates from polarization tests of raw 316L, and Ti film coated 316L (Ti@316L)

	E_{corr} (mV)	i_{corr} (μA cm^{-2})	Corrosion rate (mm/a)
316 L	− 140	5	0.057
5 μm	− 1	1.22	0.020
10 μm	− 37	0.46	0.008
17 μm	− 61	1	0.017

reaction was suppressed from the kinetics point of view. This could be inferred by the dramatic decrease in the corrosion current and the calculated corrosion rate of the Ti-coated samples.

However, two observations were noted for the anti-corrosion test. The first one was the determined values of 5 μm and 17 μm Ti corrosion current, and the corrosion rates were almost equivalent despite the varying thickness of Ti film. The corrosion rate of the 10 μm Ti-coated layer sample was the smallest, implying that the initial protection property was contributed by the presence of Ti-plated film rather than the thickness of layers, and we can conclude that the sample with 10 μm Ti coating had the best thickness condition. The corrosion potentials were determined to be − 1 mV for the 5 μm Ti layer, and − 37 mV for the 10 μm Ti-coated sample, while it was − 61 mV for the 17 μm Ti layer. The negative shift of the corrosion potential, as the layer thickness increased, indicated the loss of chemical stability during the layer growth process, which attributed to the presence of possible defects in the layer. In fact, the anti-corrosion properties were reported to deteriorate with an increase in the Ti-coated layer.

4 Conclusion

Well-stacked Ti coating was fabricated in LiCl–KCl–Ti^{x+} ($2 < x < 3$) molten salt by the constant current electroplating method, in which the Ti^{x+} ($2 < x < 3$) were prepared via the reaction between Ti^{4+} and Ti metal by mixing K_2TiF_6 and Ti metal (sponge Ti) in the melts. The formation of Ti^{x+} ($2 < x < 3$) was confirmed by ICP-AES, electrochemical monitoring technique, and XPS characterization. To optimize the electroplating parameters, the influences of temperature, current density, and deposition time were carefully investigated. The thicknesses of the obtained Ti layers were easily tuned by changing the plating parameters. Finally, the anti-corrosion behavior of the as-prepared Ti-coated 316L was tested and was found to significantly enhance the tolerance in an aggressive circumstance owing to the presence of the Ti film.

References

1. G.W. Mellors, S. Senderoff, Electrodeposition of coherent deposits of refractory metals: I niobium. J. Electrochem. Soc. **112**, 266–272 (1965). https://doi.org/10.1149/1.2423521
2. G.W. Mellors, S. Senderoff, Electrodeposition of coherent coatings of refractory metals: VII zirconium diboride. J. Elctrochem. Soc. **118**, 220–225 (1971). https://doi.org/10.1149/1.2407971
3. V.S. Protsenko, F.I. Danilov, V.O. Gordiienko, Improving hardness and tribological characteristics of nanocrystalline Cr–C films obtained from Cr(III) plating bath using pulsed electrodeposition. Int. J. Refract. Met. Hard Mater. **31**, 281–283 (2012). https://doi.org/10.1016/j.ijrmhm.2011.10.006
4. T. Zhu, W. Huang, Q. Li, Electrorefining of nickel from nicke–chromium alloy in molten LiCl–KCl. Nucl. Sci. Tech. **30**, 136 (2019). https://doi.org/10.1007/s41365-019-0656-5
5. Y. Zhang, Y.M. Song, X.H. Yu et al., Calculation and analysis of neutron and gamma shielding performance based on boron-containing stainless steel materials. Nucl. Tech. **42**, 090201 (2019). https://doi.org/10.11889/j.0253-3219.2019.hjs.42.090201 (in Chinese)
6. A. Girginov, T.Z. Tzvetkoff, M. Bojinov, Electrodeposition of refractory metals (Ti, Zr, Nb, Ta) from molten salt electrolytes. J. Appl. Electrochem. **25**, 993–1003 (1995). https://doi.org/10.1007/BF00241947
7. Q.Y. Wang, J.X. Song, G.J. Hu et al., The Equilibrium between titanium ions and titanium metal in NaCl–KCl equimolar molten salt. Metall. Mater. Trans. B **44B**, 906–913 (2013). https://doi.org/10.1007/s11663-013-9853-5
8. X.B. Zhu, Q.Y. Wang, J.X. Song et al., The equilibrium between metallic titanium and titanium ions in LiCl–KCl melts. J. Alloys Compd. **587**, 349–353 (2014). https://doi.org/10.1016/j.jallcom.2013.09.151
9. E. Chassaing, F. Basile, G. Lorthioir, Electrochemical behaviour of the titanium chlorides in various alkali chloride baths. J. Less Common Met. **68**, 153–158 (1979). https://doi.org/10.1016/0022-5088(79)90051-1
10. D. Wei, M. Okido, T. Oki, Characteristics of titanium deposits by electrolysis in molten chloride–fluoride mixture. J. Appl. Electrochem. **24**, 923–929 (1994). https://doi.org/10.1007/bf00348783
11. D. Inman, The electrode process of titanium subchlorides and electrodeposition of titanium in LiCl–KCl fused salts. Rare Met. **8**, 6–11 (1989)
12. A. Robin, J.D. Lepinay, M.J. Barbier, Electrolytic coating of titanium onto iron and nickel electrodes in the molten LiF + NaF + KF eutectic. J. Electroanal. Chem. **230**, 125–141 (1987). https://doi.org/10.1016/0022-0728(87)80137-7
13. A. Robin, R.B. Ribeiro, Pulse electrodeposition of titanium on carbon steel in the LiF–NaF–KF eutectic melt. J. Appl. Electrochem. **30**, 239–246 (2000). https://doi.org/10.1023/a:1003994100902
14. R. Baboian, D.L. Hill, R.A. Barley, Electrochemical studies on titanium in molten LiCl–KCl eutectic. Can. J. Chem. **43**, 197–205 (1965). https://doi.org/10.1139/v65-023
15. A. Robin, Influence of temperature on the reduction mechanism of Ti(III)ions on iron in the LiF–NaF–KF eutectic melt and on the electrochemical behavior of the resultant titanium coatings. Mater. Chem. Phys. **89**, 438–444 (2005). https://doi.org/10.1016/j.matchemphys.2004.10.001
16. D.M. Ferry, G.S. Picard, Impedance spectroscopy of the Ti(IV)/Ti(III) redox couple in the molten LiCl–KCl eutectic melt at 470°C. J. Appl. Electrochem. **20**, 125–131 (1990). https://doi.org/10.1007/BF01012481
17. H.D. Jiao, J.X. Wang, L. Zhang et al., Electrochemically depositing titanium(III) ions at liquid tin in a NaCl–KCl melt. RSC Adv. **5**, 62235–62240 (2015). https://doi.org/10.1039/C5RA08909C
18. C.C. Tang, X.J. Yu, J.S. Chen et al., Preparation of titanium by electrochemical reduction of titanium dioxide powder in molten $SrCl_2$–KCl. J. Alloys Compd. **684**, 699–706 (2016). https://doi.org/10.1016/j.jallcom.2016.05.206
19. H. Takamura, I. Ohno, H. Numata, Smooth and electrodeposition of titanium from LiCl–KCl–$TiCl_3$ melt. J. Jpn. Inst. Met. **60**, 388–397 (1996). https://doi.org/10.2320/jinstmet1952.60.4388
20. G.S. Chen, M. Okido, T. Oki, Electrochemical studies of titanium ions (Ti^{4+}) in equimolar KCl–NaCl molten salts with 1 wt% K_2TiF_6. Electrochim. Acta **32**, 1637–1642 (1987). https://doi.org/10.1016/0013-4686(87)90017-x
21. G.S. Chen, M. Okido, T. Oki, Electrochemical studies of titanium in fluoride–chloride molten salts. J. Appl. Electrochem. **18**, 80–85 (1988). https://doi.org/10.1007/bf01016208
22. J.X. Song, J.S. Xiao, H.M. Zhua, Electrochemical behavior of titanium ions in various molten alkali chlorides. J. Electrochem. Soc. **164**, 321–325 (2017). https://doi.org/10.1149/2.0781712jes
23. S.R. Chen, G. Xie, X.F. Zhang, Research on titanium plating in NaCl–KCl melting system. Rare Met. Mat. Eng. **6**, 471–474 (2001). https://doi.org/10.3321/j.issn:1002-185X.2001.06.017
24. Q.Q. Yang, G.K. Liu, B.L. Fang, Effects of concentration and average valence of titanium subchlorides on the electrocrystallization of titanium. Acta Metall. Sin. **16**, 365–367 (1980)
25. J.X. Song, X.X. Huang, J.Y. Wu et al., Electrochemical behaviors of Ti(III) in molten NaCl–KCl under various contents of fluoride. Electrochim. Acta **256**, 252–258 (2017). https://doi.org/10.1016/j.electacta.2017.10.058
26. L. Zhang, J. Zhu, Y. Song et al., Influence of pulsed parameters on titanium electrodeposited from LiCl–NaCl–KCl–TiClx molten salt. Chin. J. Nonferrous Met. **27**, 1068–1074 (2017). https://doi.org/10.19476/j.ysxb.1004.0609.2017.05.026
27. T.C. Yuan, Q.G. Weng, Z.H. Zhou et al., Preparation of high-purity titanium by molten-salt electrolysis process. Adv. Mater. Res. **284**, 1477–1482 (2011)
28. D.L. Li, Y.R. Zhao, G.J. Yang, Key technology and industrialization of high purity titanium by molten salt electrolysis. Chin.

Manganese Ind. **34**, 91–94 (2016). https://doi.org/10.14101/j.cnki.issn.1002-4336.2016.03.025
29. Q.G. Weng, R.D. Li, T.C. Yuan et al., Valence states, impurities and electrocrystallization behaviors during molten salt electrorefining for preparation of high-purity titanium powder from sponge titanium. Trans. Nonferrous Met. Soc. China **24**, 553–560 (2014). https://doi.org/10.1016/S1003-6326(14)63095-8
30. Q.Q. Yang, G.K. Liu, Electrochemical behavior of titanium subchlorides in NaCl–LiCl and LiCl–KCl melt. Chem. Res. Chin. Univ. **5**, 215–220 (1984)
31. J.X. Song, Q.Y. Wang, J.H. Guo et al., Equilibrium between titanium ions and high-purity titanium electrorefining in a NaCl–KCl melt. J. Miner. Met. Mater. **21**, 660–665 (2014). https://doi.org/10.1007/s12613-014-0955-0
32. I.A. Menzies, D.L. Hill, G.J. Hills et al., The mechanism of the electrodeposition of titanium from fused salts. J. Electroanal. Chem. **1**, 161–170 (1959). https://doi.org/10.1016/0022-0728(59)80025-5
33. V.V. Malyshev, D.B. Shakhnin, Titanium coating on carbon steel direct-current and inpulsive electrodeposition. Mater. Sci. **50**, 80–91 (2014). https://doi.org/10.1007/s11003-014-9694-7
34. Q.G. Weng, Z.H. Zhou, H.B. Lin et al., Preparation of high-purity titanium powder by molten-salts electrolysis. Mater. Sci. Eng. Powder Metall. **15**, 70–73 (2010)
35. X.B. Wang, D.W. Long, T.J. Zhu et al., Electrochemical behavior of Ln ~ (3 +) in LnF_3–LiCl–KCl molten salt system. Nucl. Tech. **41**, 060301 (2018). https://doi.org/10.11889/j.0253-3219.2018.hjs.41.060301 (in Chinese)
36. T.H. Yang, Y. Luo, H.Y. Fu et al., The influence of fluorides on the distillation behaviors of molten LiCl–KCl. Nucl. Tech. **41**, 120301 (2018). https://doi.org/10.11889/j.0253-3219.2018.hjs.41.120301 (in Chinese)
37. Y.S. Chen, J. Tian, H.H. Zhu et al., Experimental study on turbulent convective heat transfer of molten salts in circular tubes. Nucl. Tech. **42**, 040601 (2019). https://doi.org/10.11889/j.0253-3219.2019.hjs.42.040601 (in Chinese)
38. B.N. Popov, M.C. Kimble, R.E. White et al., Electrochemical behavior of titanium(II) and titanium(III) compounds in molten lithium chloride/potassium chloride eutectic melts. J. Appl. Electrochem. **21**, 351–357 (1991). https://doi.org/10.1007/BF01020221
39. F. Lantelme, A. Salmi, Electrochemistry of titanium in NaCl–KCl mixtures and influence of dissolved fluoride ions. J. Electrochem. Soc. **142**, 3451–3456 (1995). https://doi.org/10.1149/1.2050003
40. J.X. Song, Q.Y. Wang, J.Y. Wu et al., The influence of fluoride ions on the equilibrium between titanium ions and titanium metal in fused alkali chloride melts. Faraday Dicuss. **190**, 421–432 (2016). https://doi.org/10.1039/C6FD00007j
41. G.S. Chen, M. Okido, T. Oki, Electrochemical studies of the reaction between titanium metal and titanium ions in the KCl–NaCl molten salt system at 973 K. J. Appl. Electrochem. **17**, 849–856 (1987). https://doi.org/10.1007/bf01007823
42. L.P. Polyakova, P.T. Stangrit, E.G. Polyakov, Electrochemical study of titanium in chloride–fluoride melts. Electrochim. Acta **31**, 159–161 (1986). https://doi.org/10.1016/0013-4686(86)87102-X
43. F. Lantelme, K. Kuroda, A. Barhoun, Electrochemical and thermodynamic properties of titanium chloride solutions in various alkali chloride mixtures. Electrochim. Acta **44**, 421–431 (1980). https://doi.org/10.1016/S0013-4686(98)00168-6